International Journal of Mass Spectrometry 277 (2008) 62–69

Contents lists available at ScienceDirect

International Journal of Mass Spectrometry

journal homepage: www.elsevier.com/locate/ijms

Negative ion mass spectra of some phenalenone derivatives

N.L. Asfandiarov*, S.A. Pshenichnyuk, V.G. Lukin, A.S. Vorob'ev, A.I. Fokin

Institute of Physics of Molecules and Crystals, Ufa Research Center of RAS, October Prospect, 151, Ufa 450075, Russia

ARTICLE INFO

Article history:
Received 26 March 2008
Received in revised form 11 August 2008
Accepted 11 August 2008
Available online 20 August 2008

Keywords:
Negative ion
Autodetachment lifetime
Dissociation
Metastable ions

ABSTRACT

Temperature dependence of the negative ion mass spectra (NIMS) of six phenalenone derivatives has been investigated using a mass spectrometer with the static magnetic field mass analyzer. The dissociative attachment cross-section and the mean lifetime of the molecular NI's decreases approximately exponentially with the temperature rising, and the dissociative attachment cross-section of fragment ions generally increases with temperature. The mean lifetime of the molecular anions is at least tens of microseconds for all the investigated compounds.

1. Introduction

Some organic compounds, e.g. nitrobenzene [1] and anthraquinone derivatives [2], may produce long-lived molecular negative ions (MNI) having a dissociation decay channel at low electron energies. Their NIMS have peaks at the molecular mass what proves that the dissociation proceeds on a time scale comparable with the time of flight through a mass spectrometer—tens of microseconds. The mechanism of this phenomenon is not yet fully understood what motivated our search for compounds producing metastable MNIs. Phenalenone derivatives are widely distributed in nature [3,4]. Some of them exhibit antibiotic activity [5]. They are studied as environmental contaminants, as coal hydrogenation byproducts, as precursors to fullerenes [6], and as monomers for the synthesis of electroconductive polymers. Halogen-substituted phenalenone derivatives are used as laser dyes.

When a molecule captures an electron the resulting anion has an excess energy which is equal to the electron affinity plus the impinging electron energy plus the initial vibrational energy of the molecule [7,8]. Statistically, this last value is proportional to the gas temperature [9]. If the anion initially survives a time of order a molecular vibration period, the excess energy may be redistributed among internal degrees of freedom of the ion. For large molecules, the number of degrees of freedom allows thermodynamical description, and the resulting ion state may be characterized by an effective temperature [9,10].

The further evolution of the ion may proceed through the autodetachment of the electron and/or the dissociation:

$$M^{-*} \xrightarrow{k_a} M + e^-,$$

$$M^{-*} \xrightarrow{k_d} [M - R] + R^-,$$

here M stands for the molecule, and R for an appropriate fragment. Under the above conditions, one can expect that the ion's life time is long enough, and the rate constants, k_a and k_d, have an Arrhenius-type behavior with the ion temperature. It should be noted, however, that the calculation of this temperature is, generally, a very complicated problem [9,10]. Nevertheless, within this framework many useful conclusions may be made even on a qualitative level.

A negative ion mass spectrometer has an observation window of tens of microseconds. For sufficiently long-lived ions, a data gathered in a single experiment contains enough information to estimate different rate constants even when competing reaction channels are present. Analysis of dependence of these values on the target gas temperature makes possible to conclude on the validity of the above model and assess a possible contribution of repulsive electronic terms to the ion dynamics.

Phenalenone derivatives are large aromatic molecules with a positive electron affinity which makes them promising objects for this kind of study. To our best knowledge, these compounds have not yet been investigated by means of the NIMS.

* Corresponding author. Tel.: +7 347 2313538; fax: +7 347 2313538.
E-mail address: nail@anrb.ru (N.L. Asfandiarov).

1387-3806/$ – see front matter © 2008 Elsevier B.V. All rights reserved.
doi:10.1016/j.ijms.2008.08.008

Table 1
NI mass spectra of phenalenone derivatives

m/z	E_{max} (eV)	Relative intensity	Intensity (%)	Integral intensity	Lifetime (μs)	Structure
2,6-Br_2-phenalenone. Ion source temperature 110 °C. EA_a = 1.539 eV						
338	0.14	262	100	9125	~1000 (0.0)	M^-
					720 (0.14 eV)	
79	0.5	120	45.8	6514		Br^-
	~2.1	12	4.6			
	~3	8	3.05			
m^* = 18.46	~0.3	0.3	0.11	13.27		$M^- \rightarrow Br^-$
M^0	~0.33	3.7	1.4	163		$M^- \rightarrow M^0 + e^-$
2,6-Br_2-phenalenone. Ion source temperature 140 °C						
338	0.14	165	100	5376	~800 (0.0)	M^-
					560 (0.14 eV)	
79	0.46	110	66.7	6202		Br^-
	~2.1	12	7.3			
	~3	8	4.8			
m^* = 18.46				12.66		$M^- \rightarrow Br^-$
M^0	~0.3	3.4	2.1	127		$M^- \rightarrow M^0 + e^-$
2,6-Br_2-phenalenone. Ion source temperature 170 °C						
338	0.11	135	94.4	4061	550 (0.0)	M^-
					390 (0.14 eV)	
79	0.37	143	100	7829		Br^-
	~2.1	12	8.4			
	~3	8	5.6			
m^* = 18.46				12.65		$M^- \rightarrow Br^-$
M^0	~0.22	3.4	2.4	124		$M^- \rightarrow M^0 + e^-$
2,6-Br_2-phenalenone. Ion source temperature 200 °C						
338	0.11	100	54.6	3214	~400 (0.0)	M^-
					290 (0.14 eV)	
79	0.28	183	100	9773		Br^-
	~2.1	12	6.6			
	~3	8	4.4			
m^* = 18.46				12.19		$M^- \rightarrow Br^-$
M^0	~0.15	3.2	1.7	115		$M^- \rightarrow M^0 + e^-$

m/z	E_{max} (eV)	Relative intensity	Intensity (%)	Integral intensity	Lifetime (μs)	Structure
2-Br-phenalenone. Ion source temperature 90 °C. EA_a = 1.307 eV						
258	0.22	71	49	2431	355 (0.0)	M^-
					220 (0.22 eV)	
79	0.52	145	100	7965		Br^-
	~3	17	11.7			
m^* = 24.19	~0.35	0.4	0.28	14.61		$M^- \rightarrow Br^-$
M^0	~0.34	2.57	1.8	89.89		$M^- \rightarrow M^0 + e^-$
2-Br-phenalenone. Ion source temperature 110 °C						
258	0.19	51	42.9	1717	320 (0.0)	M^-
					235 (0.22 eV)	
79	0.48	119	100	6791		Br^-
	~3	17	14.3			
m^* = 24.19	~0.35	0.23	0.19	8.93		$M^- \rightarrow Br^-$
M^0	~0.34	1.92	1.6	64.17		$M^- \rightarrow M^0 + e^-$
2-Br-phenalenone. Ion source temperature 170 °C						
258	0.16	32	19.2	966	230 (0.0)	M^-
					160 (0.22 eV)	
79	0.38	167	100	9333		Br^-
	~3	17	10.2			
m^* = 24.19	~0.36	0.22	0.13	10.97		$M^- \rightarrow Br^-$
M^0	~0.23	1.35	0.81	44.67		$M^- \rightarrow M^0 + e^-$
2-Br-phenalenone. Ion source temperature 200 °C						
258	0.14	20	8.8	579	160 (0.0)	M^-
					110 (0.22 eV)	
79	0.33	227	100	12134		Br^-
	~3	17	7.5			
m^* = 24.19	~0.25	0.19	0.08	7.60		$M^- \rightarrow Br^-$
M^0	~0.18	1.13	0.5	34.46		$M^- \rightarrow M^0 + e^-$

m/z	E_{max} (eV)	Relative intensity	Intensity (%)	Integral intensity	Lifetime (μs)	Structure
2-NO_2-phenalenone. Ion source temperature 110 °C. EA_a = 1.818 eV						
225	0.01	1176	100	68802	~50000 (0.0)	M^-
	0.34	1157	98.4		15700 (0.34 eV)	
195	2.14	16.8	1.4	1599		$(M\text{-}NO)^-$
46	2.33	371	31.5			NO_2^-
				60692		

Table 1 (*Continued*)

m/z	E_{max} (eV)	Relative intensity	Intensity (%)	Integral intensity	Lifetime (μs)	Structure
	2.95	351	29.8			
m^* = 169.0	1.5	0.17	0.014	11.38		$M^- \rightarrow NO + (M\text{-}NO)^-$
m^* = 9.4	1.6	0.15	0.013	8.29		$M^- \rightarrow NO_2^- + (M\text{-}NO_2)$
M^0	~0.8	0.72	0.06	191		$M^- \rightarrow M^0 + e^-$
2-NO_2-phenalenone. Ion source temperature 140 °C						
225	0.01	809	100	45536	~40000 (0.0)	M^-
	0.34	783	96.8		~9080 (0.34 eV)	
195	2.13	12.6	1.6	1295		$(M\text{-}NO)^-$
46	2.32	106	13.1	17951		NO_2^-
	3.0	100	12.4			
m^* = 169.0	1.4	0.1	0.012	9.33		$M^- \rightarrow NO + (M\text{-}NO)^-$
m^* = 9.4	1.3	0.1	0.012	6.76		$M^- \rightarrow NO_2^- + (M\text{-}NO_2)$
M^0	~1	2.2	0.27	146		$M^- \rightarrow M^0 + e^-$
2-NO_2-phenalenone. Ion source temperature 170 °C						
225	0.01	578	95.7	32409	~15000 (0.0)	M^-
	0.3	604	100		~3770 (0.3 eV)	
195	1.95	9.1	1.5	1029		$(M\text{-}NO)^-$
46	2.25	92	15.2	15282		NO_2^-
	3.2	75	12.4			
m^* = 169.0	0.95	0.1	0.017	9.33		$M^- \rightarrow NO + (M\text{-}NO)^-$
m^* = 9.4	1.2	0.1	0.017	6.95		$M^- \rightarrow NO_2^- + (M\text{-}NO_2)$
M^0	~0.7	2.3	0.38	155		$M^- \rightarrow M^0 + e^-$
2-NO_2-phenalenone. Ion source temperature 200 °C						
225	0.01	428	93.0	23948	~5000 (0.0)	M^-
	0.3	460	100		~2230 (0.3 eV)	
195	0.67	4.3	0.93	824		$(M\text{-}NO)^-$
	2.05	5.9	1.3			
46	0.75	24	5.2	14400		NO_2^-
	2.4	77	16.7			
m^* = 169.0	0.7	0.1	0.02	8.57		$M^- \rightarrow NO + (M\text{-}NO)^-$
m^* = 9.4	0.9	0.1	0.02	7.13		$M^- \rightarrow NO_2^- + (M\text{-}NO_2)$
M^0	~0.7	2.9	0.63	161		$M^- \rightarrow M^0 + e^-$

m/z	E_{max} (eV)	Relative intensity	Intensity (%)	Integral intensity	Lifetime (μs)	Structure
3-Br-phenalenone. Ion source temperature 80 °C. EA_a = 1.297 eV						
258	0.03	569	39.7	16059	~170 (0.0)	M^-
	0.22_{sh}	459	38.9		112 (0.22 eV)	
79	0.45	1180	100	65235		Br^-
	~2.6	90	7.6	7853		
m^* = 24.19	~0.22	3.45	0.29	128		$M^- \rightarrow Br^-$
M^0	~0.16	20	1.69	697		$M^- \rightarrow M^0 + e^-$
3-Br-phenalenone. Ion source temperature 110 °C						
258	0.06	406	33.6	11126	~150 (0.0)	M^-
	0.23_{sh}	273	22.6		96 (0.22 eV)	
79	0.39	1210	100	68644		Br^-
	~2.6	90	7.4	6645		
m^* = 24.19	~0.17	2.9	0.24	103		$M^- \rightarrow Br^-$
M^0	~0.13	16	1.3	505		$M^- \rightarrow M^0 + e^-$
3-Br-phenalenone. Ion source temperature 140 °C						
258	0.04	288	20.5	7305	~125 (0.0)	M^-
					78 (0.22 eV)	
79	0.28	1406	100	79686		Br^-
	~2.6	90	6.4	7073		
m^* = 24.19	~0.1	2.8	0.2	90		$M^- \rightarrow Br^-$
M^0	~0.09	14	1.0	410		$M^- \rightarrow M^0 + e^-$
3-Br-phenalenone. Ion source temperature 170 °C						
258	0.03	188	10.5	4283	~100 (0.0)	M^-
					64 (0.22 eV)	
79	0.24	1792	100	96240		Br^-
	~2.6	90	5.0	5042		
m^* = 24.19	~0.08	2.3	0.13	60		$M^- \rightarrow Br^-$
M^0	~0.06	10	0.56	285		$M^- \rightarrow M^0 + e^-$

Table 1 (*Continued*)

m/*z*	E_{max} (eV)	Relative intensity	Intensity (%)	Integral intensity	Lifetime (μs)	Structure
3-Br-phenalenone. Ion source temperature 200 °C						
258	0.04	114	4.9	2648	~90 (0.0) 64 (0.22 eV)	M^-
79	0.17	2340	100	121009		Br^-
	~2.6	90	3.8	7269		
m^* = 24.19	~0.01	1.6	0.068	42		$M^- \rightarrow Br^-$
M^0	~0.04	7.4	0.32	177		$M^- \rightarrow M^0 + e^-$

m/*z*	E_{max} (eV)	Relative intensity	Intensity (%)	Integral intensity	Lifetime (μs)	Structure
5-Br-phenalenone. Ion source temperature 80 °C. EA_a = 1.284 eV						
258	0.03	943	100	31623	~700 (0.0) 187 (0.29 eV)	M^-
	0.29_{sh}	707	75.0			
79	0.58	520	55.1	27332		Br^-
	~2.4	42	4.5	3348		
m^* = 24.19	~0.4	2.44	0.26	87		$M^- \rightarrow Br^-$
M^0	~0.4	17	1.8	600		$M^- \rightarrow M^0 + e^-$
5-Br-phenalenone. Ion source temperature 110 °C						
258	0.06	586	99.7	18282	~400 (0.0) 140 (0.29 eV)	M^-
	0.26_{sh}	457	77.7			
79	0.51	588	100	29854		Br^-
	~2.4	40	6.8	2038		
m^* = 24.19	~0.33	2.3	0.39	82		$M^- \rightarrow Br^-$
M^0	~0.3	14	5.88	526		$M^- \rightarrow M^0 + e^-$
5-Br-phenalenone. Ion source temperature 140 °C						
258	0.07	398	57.5	12115	~200 (0.0) 90 (0.29 eV)	M^-
	0.28_{sh}	262	37.9			
79	0.42	692	100	36107		Br^-
	~2.4	40	5.8	2161		
m^* = 24.19	~0.24	2.1	0.3	77		$M^- \rightarrow Br^-$
M^0	~0.22	12	1.7	445		$M^- \rightarrow M^0 + e^-$
5-Br-phenalenone. Ion source temperature 170 °C						
258	0.07	264	32.0	7514	~150 (0.0) 83 (0.29 eV)	M^-
	0.25_{sh}	176	21.4			
79	0.37	824	100	43888		Br^-
	~2.4	40	4.9	2596		
m^* = 24.19	~0.18	1.54	0.19	54		$M^- \rightarrow Br^-$
M^0	~0.14	9.8	1.2	336		$M^- \rightarrow M^0 + e^-$
5-Br-phenalenone. Ion source temperature 200 °C						
258	0.07	162	15.5	4378	~120 (0.0) 80 (0.29 eV)	M^-
	0.25_{sh}	108	10.3			
79	0.31	1045	100	54316		Br^-
	~2.4	40	3.8	3443		
m^* = 24.19	~0.12	1.18	0.11	40		$M^- \rightarrow Br^-$
M^0	~0.09	7.7	0.74	237		$M^- \rightarrow M^0 + e^-$

m/*z*	E_{max} (eV)	Relative intensity	Intensity (%)	Integral intensity	Lifetime (μs)	Structure
6-Br-phenalenone. Ion source temperature 80 °C. EA_a = 1.329 eV						
258	0.01	828	100	24283	~400 (0.0) 178 (0.22 eV)	M^-
	0.22_{sh}	552	66.7			
79	0.56	508	61.4	25403		Br^-
	~2.5	37	4.5	3443		
m^* = 24.19	~0.36	1.63	0.2	66		$M^- \rightarrow Br^-$
M^0	~0.28	12.4	1.5	517		$M^- \rightarrow M^0 + e^-$
6-Br-phenalenone. Ion source temperature 110 °C						
258	0.03	512	100	14012	~300 (0.0) 140 (0.22 eV)	M^-
	0.22_{sh}	305	59.6			
79	0.52	433	84.6	22185		Br^-
	~2.5	37	7.2	2533		
m^* = 24.19	~0.31	1.45	0.28	61		$M^- \rightarrow Br^-$
M^0	~0.20	8.7	1.7	348		$M^- \rightarrow M^0 + e^-$
6-Br-phenalenone. Ion source temperature 140 °C						
258	0.01	392	81.7	9647	~200 (0.0) 101 (0.22 eV)	M^-
	0.21_{sh}	199	41.5			
79	0.47	480	100	26410		Br^-
	~2.5	37	7.7	2772		
m^* = 24.19	~0.19	1.16	0.24	46		$M^- \rightarrow Br^-$
M^0	~0.10	8.3	1.7	300		$M^- \rightarrow M^0 + e^-$
6-Br-phenalenone. Ion source temperature 170 °C						
258	0.02	285	50.1	6455	~150 (0.0) 73 (0.22 eV)	M^-
	0.22_{sh}	118	20.7			

Table 1 (*Continued*)

m/z	E_{max} (eV)	Relative intensity	Intensity (%)	Integral intensity	Lifetime (μs)	Structure
79	0.39	569	100	32641		Br^-
	~2.5	37	6.5	2622		
m^* = 24.19	~0.08	1.3	0.23	45		$M^- \rightarrow Br^-$
M^0	~0.08	8.4	1.5	252		$M^- \rightarrow M^0 + e^-$
6-Br-phenalenone. Ion source temperature 200 °C						
258	0.04	183	25.6	3802	~120 (0.0) 67 (0.22 eV)	M^-
	0.2_{sh}	70	9.8			
79	0.33	714	100	40276		Br^-
	~2.5	37	5.2	2634		
m^* = 24.19	~0.08	1.3	0.18	36		$M^- \rightarrow Br^-$
M^0	~0.06	6.8	0.95	175		$M^- \rightarrow M^0 + e^-$

Integral intensity means the peak area. Lifetimes, calculated according to formula (3), are listed for zero electron energy, the second values are listed for the molecular NI maximum, peak energy in parentheses; EA_a means AM1 calculated ε_{LUMO} energy scaled using relation (1).

2. Experiment

The NIMS experiment was performed using a MI-1201 mass spectrometer described in details in [1]. In the mass spectrometer an electron beam passes through the ionization chamber filled with the gas-phase compound under investigation. The count of negative ions is recorded mass spectrometrically as a function of the incident electron energy. The mass spectrometer consists of a negative ion source, a 90° magnetic sector analyzer, and a secondary electron multiplier with a multiplication factor of about 10^6. The vacuum system is heatable up to 300 °C and consists of two 100 l/s oil diffusion pumps with liquid nitrogen traps. One pump is used for evacuating the chamber in which the negative ion source is located. The other one reduces the pressure in the chamber where the secondary electron multiplier is placed. The residual pressure in the vacuum system of the mass spectrometer does not exceed 1.5×10^{-8} Torr.

All electrodes of the negative ion source are made of stainless steel and coated with soot in order to reduce the reflection of electrons from the electrodes. The coating also decreases the formation of dielectric films on electrode surfaces, which may influence the electric field potentials inside the anion source. The electrons emitted from a tungsten filament are collimated by an axial magnetic field of about 80 G. The electrons with fwhm ~0.4 eV are accelerated into the collision chamber where they interact with the target gas. The pressure inside the collision chamber is kept as low as $\sim 10^{-6}$ Torr in order to ensure single-collision conditions. After passing the collision chamber, the electrons are collected by an electron trap. The electron current is about 1 μA at the electron energy of 8 eV. The full electron energy range accessible in this experiment was 0–12 eV. The negative ions are extracted from the collision chamber and accelerated to the magnetic mass analyzer by a potential difference of 4 kV. The time of flight for the SF_6^- ion (m/z = 146), from its formation in negative ion source to the detection with the secondary electron multiplier, is about 20 μs. The estimated accuracy of determination of the peak positions is ±0.1 eV.

Six phenalenone derivatives were studied: 2,6-Br_2-phenalenone (**1**); 2-Br-phenalenone (**2**); 2-NO_2-phenalenone (**3**); 3-Br-phenalenone (**4**); 5-Br-phenalenone (**5**); 6-Br-phenalenone (**6**). The numbering scheme is as follows:

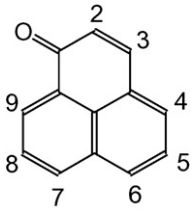

3. Results and discussion

For all the compounds a dissociative attachment was observed at low electron energies. Experimental data are listed in Table 1. Relative Intensity, column 3, stands for the maximum peak intensity of a given ion. In a column Integral Intensity we also listed total peak areas. This parameter reflects the overall production of a given type of anions in a resonance and, as the electron energy resolution in the experiment is relatively low, may be used in calculations of the anion mean lifetime, see e.g. [11].

In bromine-substituted phenalenones dissociation proceeds through C–Br bond breaking. Figs. 1 and 2 demonstrate typical temperature dependencies for different types of peaks for **1** and **2**. In the case of the 2,6-Br_2-phenalenone, a calculated energy splitting between two appropriate σ_{C-Br}^*-orbitals is about the same as the electron fwhm, and, by analogy with bromoalkanes [12], we believe either of them may capture an impinging electron.

The electron structures of compounds under study were calculated for the optimal geometry by the semiempirical AM1 method. To estimate the electron affinities, the results for ε_{LUMO} were scaled by a linear relation found by Modelli and Mussoni for the case of large aromatic compounds [13]:

$$EA_a = -0.9898\,\varepsilon_{LUMO} - 0.2539, \quad (1)$$

where EA_a is the adiabatic electron affinity. As the 6 lowest unoccupied MO for all the compounds with the only exception of one σ_{C-Br}^* MO (for monosubstituted derivatives) and two for dibromo-substituted derivatives, have π^*-type and are delocalized on aromatic rings of the anthraquinone skeleton, it is reasonable to conclude that Eq. (1) is applicable in this case. It should be noted that the σ^*-type orbitals require an altogether different scaling [14]. It may be seen in Figs. 1 and 2, that calculated positions of π^*-orbitals shown as vertical lines above the upper right panels closely correlate with maxima of the effective yield of NI. The main peak of Br^- is in a region ~0.5 eV where there are at least three unoccupied π^*-MO, what makes impossible to unambiguously connect this resonance with one of them. Scaled values of EA_a are listed in Table 1.

For the 2-nitro-phenolenone the dominant channel for dissociation is a breaking away of NO_2^-. Besides, an additional peak corresponding to the reaction

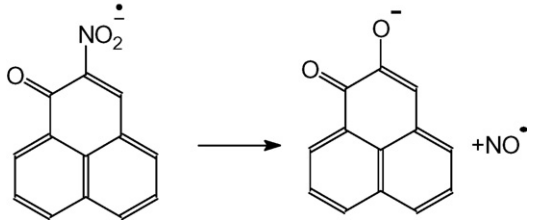

was also detected.

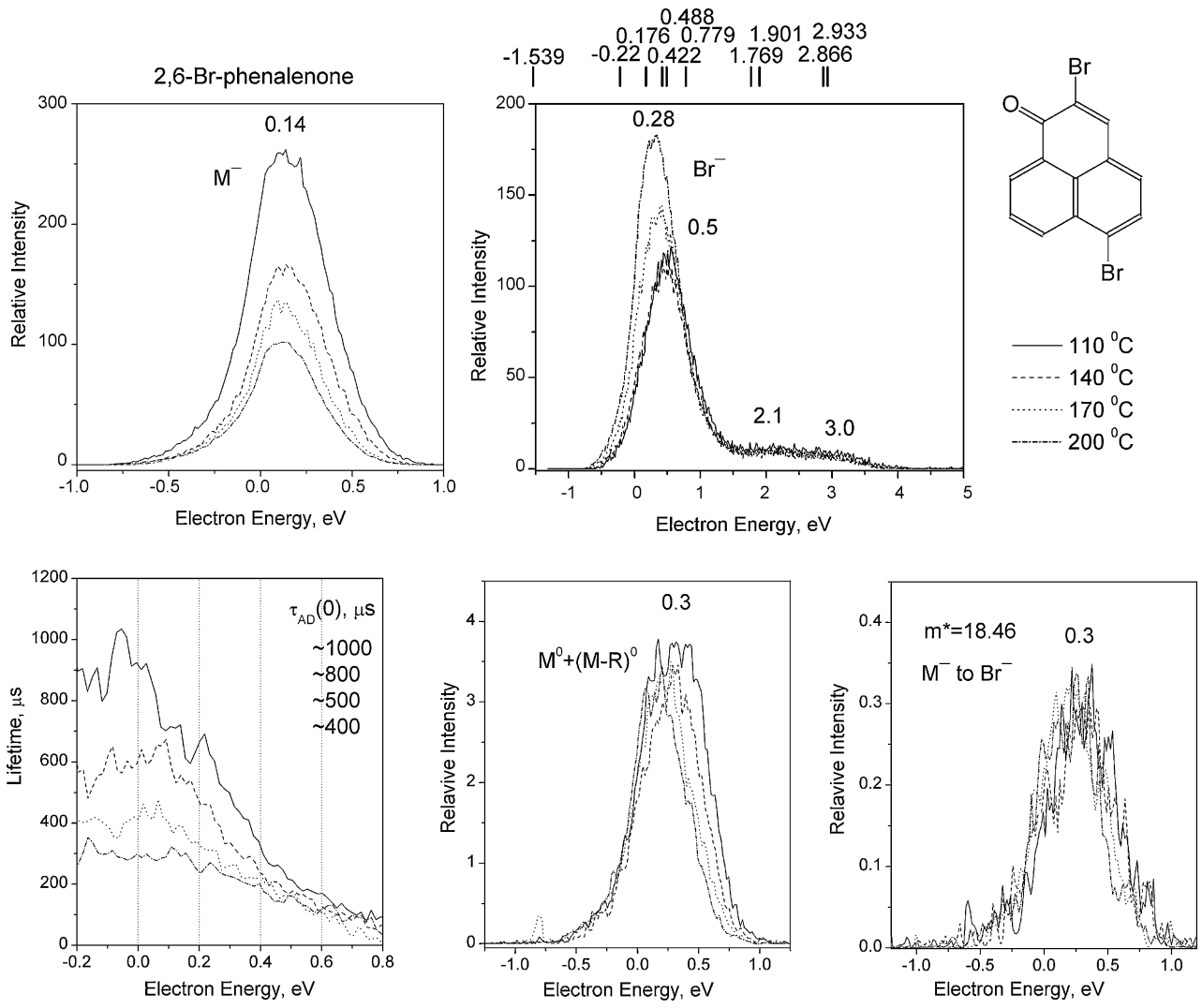

Fig. 1. Upper panels: temperature dependencies of the effective yield curves for parent and fragment ions from the 2,6-Br_2-phenalenone. Estimated energies of empty levels are shown above the right panel, see text. Lower panels: temperature dependencies of mean autodetachment lifetime; relative intensity of the neutrals and metastable ions.

The relative and integral intensities of M^- decrease approximately exponentially with the temperature rising for all the compounds under investigation. The temperature dependence of Br^- is more complicated. In contrast with the results of Rosa et al. for 1,4-chloronitrobenzene [15] dissociative cross-section of Br^- at first decreases with the temperature, and after passing a minimum (∼150 °C for **1**; ∼110 °C for **2** and **6**) increases. In **3** the intensity of NO_2^- monotonically decreases with the temperature rising. The dissociative cross-section of Br^- increases approximately exponentially with the temperature for **4** and **5**. As it will be discussed below such a behavior may result from a possible contribution of repulsive electronic terms.

To quantitatively estimate the NI lifetime, consider the timing of the experiment in more detail (see Fig. 3). The molecular anions are produced at the moment t_0 (it may be set equal to 0) in the ion source. Fragment ions from dissociation events till the time t_1 are detected as narrow peaks at their proper mass m (see middle panel of Fig. 4). Extracted from the collision chamber at moment t_1, the ions are accelerated into the first drift region. Because the fragment ions produced in this region (t_1 to t_2) retain the velocity of the molecular ions, they are detected at the nonintegral apparent mass $m^* = m^2/M$, where M stands for the molecular mass [16], and produce broader peaks. In the decay reaction, the fragments receive a transverse momentum, and, as a result, some fraction of them misses a slit of the mass analyzer. Though, the loss may not be calculated precisely and, for this reason, the count value at this mass may not be used for quantitative calculations, the real intensity is comparable with the measured one. After passing the mass analyzer at moment t_3, the ions enter the second field-free drift region. Both kinds of fragments, charged and neutral, from the dissociation of the MNIs in this region contribute to the peak at the mass M. By applying voltage to the special deflection electrodes, the ions may also be diverted from the secondary electron multiplier. In this mode only fast neutrals formed in the second drift region are counted. Given the ion mass, the time of flight for each part of the ion path may be calculated from the instrument geometry. An estimated extraction time of the ion with $m/z = 258$ (Br-phenalenone) is about $t_1 \sim 6$ μs. The flight time of this ion through the first free drift region is $t_2 - t_1 = 8$ μs at the acceleration voltage 4 kV. Ions pass magnet mass analyzer in $t_3 - t_2 = 8$ μs and the second free drift region also in $t_4 - t_3 = 8$ μs. So, the total MNI drift time from the ion source to the ion detector is about 24 μs for $m/z = 258$.

Assuming that both the dissociation and autodetachment rates are constant it is straightforward to express the ion count at mass m and the counts of all and the neutral only species at mass M through the flight times. With known values for these counts the expres-

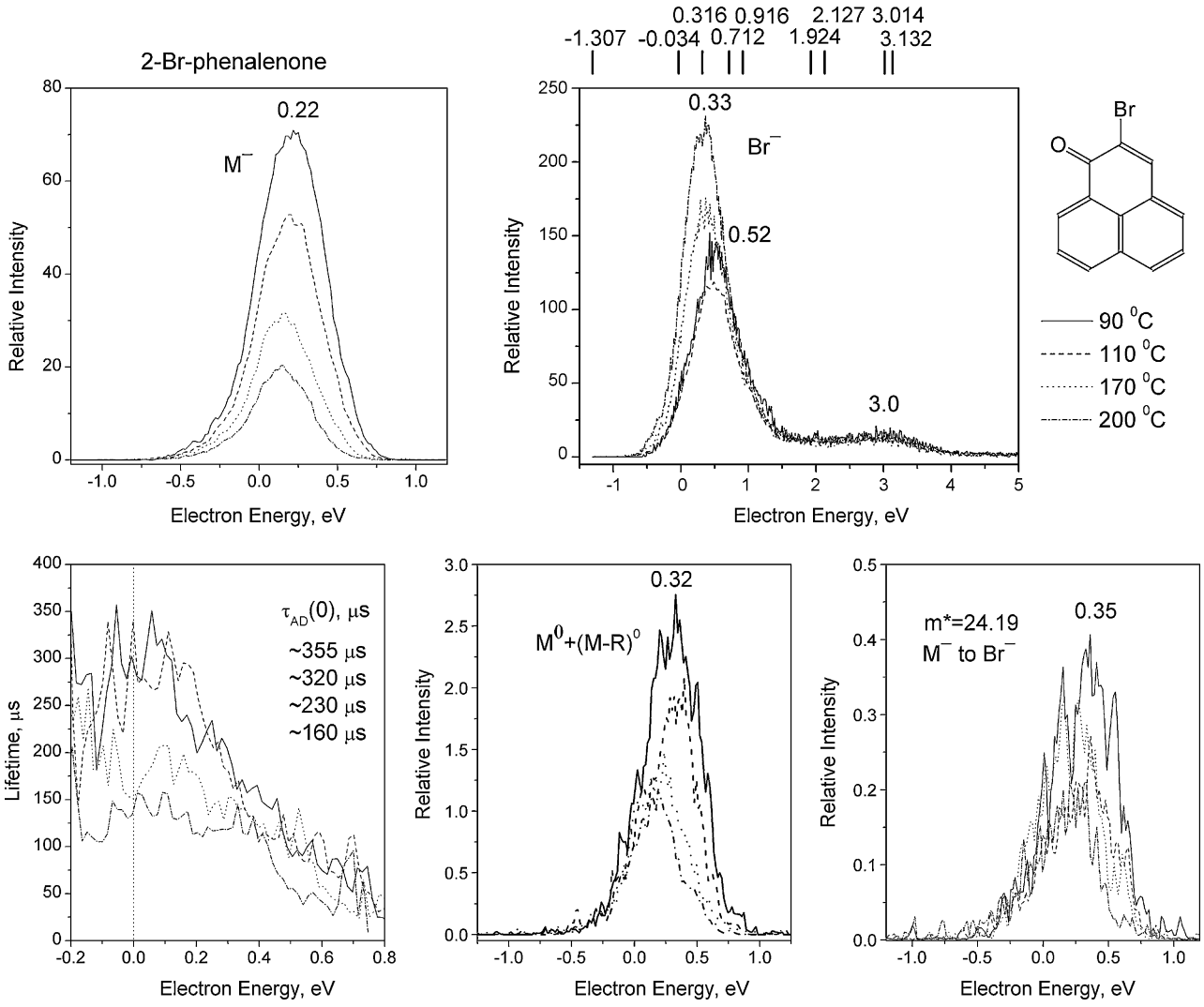

Fig. 2. Upper panels: temperature dependencies of the effective yield curves for parent and fragment ions from the 2-Br-phenalenone. Estimated energies of empty levels are shown above the right panel, see text. Lower panels: temperature dependencies of mean autodetachment lifetime; relative intensity of the neutrals and metastable ions.

sions may be solved relative to the reaction rates. As it turned out, for our experimental data this solution always give a non-physical negative value for one of the reaction rates. A simple analysis has shown that the count of the fragment ions from the ion source as compared with the counts at mass M is at least an order of magnitude too large for this approach to produce meaningful reaction rates. Therefore it may be concluded that the incompatibility of the experimental data with the assumption of the constant reaction rates indicates that a considerable part of the MNIs dissociate in the ion source on a faster timescale. The fast decay may result from the possible contribution of repulsive electronic terms in this interval of electron energies. As a probability of the capture on a repulsive term and a survival factor depend, generally, on the molecule's energy, the resulting temperature dependence of the fragment ion intensity may be rather complicated.

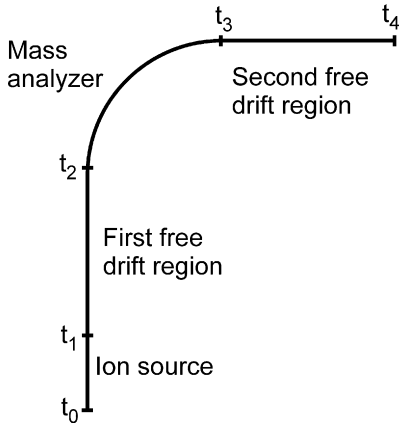

Fig. 3. Timing of the experiment, see text.

The particle counts at the mass number M depend only on the number of MNIs that survived till the moment t_3. As this time is long enough, a thermodynamical approach to their decay kinetics seems well founded. These counts are related to the reaction rates by the following expression:

$$\tau = \frac{1}{k_a + k_d} = \frac{t_4 - t_3}{\ln([M] - (k_d/(k_a + k_d))[N])/([M] - (1 + (k_d/(k_a + k_d)))[N])}, \quad (2)$$

where [M] stands for the count of all species, [N] for the count of the neutrals.

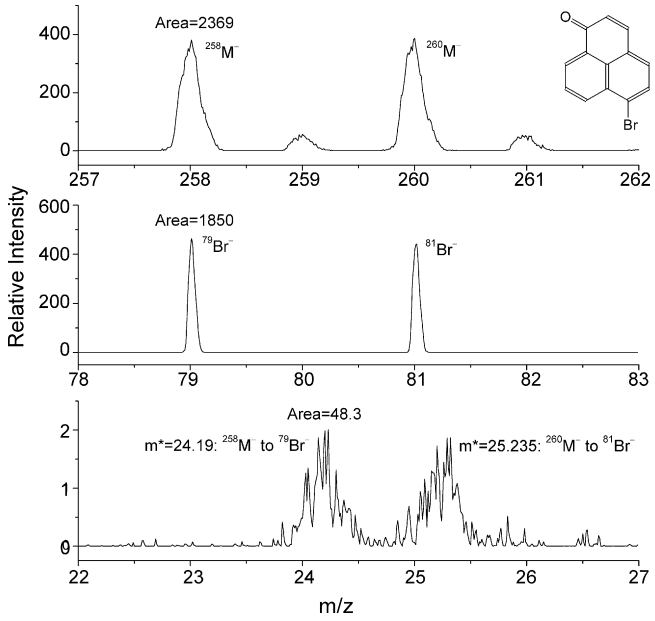

Fig. 4. NI mass spectrum of the 6-Br-phenalenone. Area means the integral over a mass peak.

The left hand side of Eq. (2) is the combined life time, τ, of the MNI in the second drift region. If no dissociation occurs in this region ($k_d = 0$), Eq. (2) reduces to the well known formula [8,17,18]

$$\tau = \frac{t_4 - t_3}{\ln[M]/[M] - [N]}. \quad (3)$$

In a general case, the lifetime cannot be accurately calculated solely from Eq. (2), but in the limit $[N] \ll [M]$ the relative contribution to the r.h.s of Eq. (2) from the unknown $k_d/k_a + k_d$ ratio is only as small as $k_d/k_a + k_d([N]/[M])^2$. From the physical point of view, this signifies that when the combined lifetime $\tau \gg (t_4 - t_3)$, the dissociation events producing one charged and one neutral species and the autodetachment events producing only a neutral species – the molecule – became indiscernible on the background of survived charged MNIs. For our data this uncertainty is well within the experimental error, so the lifetimes listed in Table 1 were calculated using Eq. (3).

The peaks at the apparent mass m^* are the direct evidence that the dissociation takes place not only within the ion source but also in the first drift region, therefore it contributes to the value of τ. As it was already pointed out, the unknown efficiency of ion registration at this mass precludes quantitative estimations using these data. Nevertheless, within any reasonable range of this uncertainty, the observed values of $[N]$ cannot be attributed only to the dissociation of MNIs in the second drift region. This is evidence that the electron autodetachment from the MNIs makes a considerable contribution to the combined lifetime in this region.

4. Conclusions

All the six phenalenone derivatives produce at the low electron energies the metastable molecular anions which then either dissociate producing fragment ions or detach the captured electron. The dissociation kinetics may not be characterized by a single lifetime value but rather have a set of them, the longest being at least in the tens of microseconds range. The autodetachment lifetime has a comparable value. Only the combined lifetime relative to both the processes may be calculated from the experimental data. Most probably, the MNI is initially formed in different states with different lifetimes [19].

The temperature dependencies of the spectra, while generally following the predictions of the thermodynamical description of the ion kinetics [9,11], also exhibit some features that may be attributed to the existence of different initial states of the MNI.

Acknowledgements

This work in part was supported by Russian Foundation for Basic Research, Grant 06-03-32059. N.L.A. wishes to thank The National Scholarship Program of the Slovak Republic, visiting Grant C-3, 15 May 2007.

References

[1] N.L. Asfandiarov, S.A. Pshenichnyuk, I.A. Pshenichnyuk, V.G. Lukin, A. Modelli, Š. Matejčik, Int. J. Mass Spectrom. (2007) 22, 264/1.
[2] N.L. Asfandiarov, V.S. Fal'ko, V.G. Lukin, E.P. Nafikova, S.A. Pshenichnyuk, A.I. Fokin, G.S. Lomakin, Yu.V. Chizov, Rapid Commun. Mass Spectrom. 15 (2001) 1869.
[3] R.H. Binks, J.R. Greenham, J.G. Luis, S.R. Gowen, Phytochemistry 45 (1997) 47.
[4] F.H. Stodola, K.B. Raper, D.I. Fennell, Nature 167 (1951) 773.
[5] N. Narasimhachari, K.S. Gopalkrishnam, R.H. Haskins, L.C. Vining, Can. J. Microbiol. 9 (1963) 134.
[6] S. Pogodin, I. Agranat, Org. Lett. 1 (1999) 1387.
[7] E. Illenberger, B.M. Smirnov, Uspekhi Fiz. Nauk (Rus.) 168 (1998) 731.
[8] L.G. Christophorou, M.W. Grant, D.L. McCorkle, Adv. Chem. Phys. 36 (1977) 413.
[9] C.E. Klots, Int. Rev. Phys. Chem. 15 (1996) 205.
[10] Š. Matejčík, T.D. Märk, P. Španěl, D. Smith, T. Jaffke, E. Illenberger, J. Chem. Phys. 102 (1995) 2516.
[11] E.C.M. Chen, J.R. Wiley, C.F. Batten, W.E. Wentworth, J. Phys. Chem. 98 (1994) 88.
[12] S.A. Pshenichnyuk, N.L. Asfandiarov, P.D. Burrow, Rus. Chem. Bull. 56 (2007) 1.
[13] A. Modelli, L. Mussoni, Chem. Phys. 332 (2007) 367.
[14] K. Aflatooni, G.A. Gallup, P.D. Burrow, J. Phys. Chem. A 104 (2000) 7359.
[15] A. Rosa, W. Barszczewska, D. Nandi, V. Ashok, S.V.K. Kumar, E. Krishnakumar, F. Brüning, E. Illenberger, Chem. Phys. Lett. 342 (2001) 536.
[16] J.H. Beynon, Mass Spectrometry and its Applications to Organic Chemistry, Elsevier Publishing Co., Amsterdam/London/New York/Princeton, 1960.
[17] A. Hadjiantoniu, L.G. Christophorou, J.G. Carter, J. Chem. Soc., Faraday Trans. II 69 (1973) 1691.
[18] V.I. Khvostenko. Negative Ion Mass Spectrometry in Organic Chemistry. Nauka. Moscow, 1981.
[19] K. Graupner, T.A. Field, A. Mauracher, P. Scheier, A. Bacher, S. Denifl, F. Zappa, T.D. Märk, J. Chem. Phys. 128 (2008) 104304.